Effect of the Mixing Sequence on the Morphology and Properties of a Polypropylene/Polydimethylsiloxane/ Nano-SiO_2 Ternary Composite

K. Prakashan, A. K. Gupta, S. N. Maiti

Centre for Polymer Science and Engineering, Indian Institute of Technology Delhi, New Delhi 110016, India

Received 23 December 2007; accepted 11 April 2008
DOI 10.1002/app.28544
Published online 17 July 2008 in Wiley InterScience (www.interscience.wiley.com).

ABSTRACT: Ternary composites of polypropylene (PP), polydimethylsiloxane (PDMS) elastomer, and nano-SiO_2, prepared with three different mixing sequences, were studied for dispersion morphology and its effect on the crystallization of PP and the mechanical properties. The mixing sequence produced a significant effect on the dispersion morphology and, thereby, on the mechanical properties of the composites. A two-step mixing sequence, in which nano-SiO_2 was added in the second step to the PP/PDMS binary system, produced a significant encapsulation of nano-SiO_2 by PDMS, and this, in turn, resulted in the poor modulus and impact strength of the composite. A one-step mixing sequence of all three components produced a separated dispersion of PDMS and nano-SiO_2 phases in the PP matrix with the occurrence of a fine band of nano-SiO_2 particles at the boundaries of the PDMS domains and the presence of some nano-SiO_2 filler particles inside the PDMS domains. This one-step mixing sequence produced an improvement in the tensile modulus but a decrease in the impact strength with increasing nano-SiO_2 content. In the third sequence of mixing, which involved a two-step mixing sequence through the addition of PDMS in the second step to the previously prepared PP/nano-SiO_2 binary system, the morphology of the dispersion showed separately dispersed PDMS and nano-SiO_2 phases with a loose network of nano-SiO_2 particles surrounding the PDMS domains. This latter series of ternary composites had the highest impact strength and exhibited high shear deformation under tensile and impact conditions. © 2008 Wiley Periodicals, Inc. J Appl Polym Sci 110: 1457–1468, 2008

Key words: crystallization; dispersions; mechanical properties; nanocomposites; poly(propylene) (PP)

INTRODUCTION

Ternary composites consisting of polypropylene (PP) as matrix, an elastomer, and a rigid particulate filler as minor components have been an attractive area of study because of the possibility of the simultaneous improvement of toughness and stiffness. The properties of such ternary composites are dependent on the relative dispersion of the additive components in the matrix. Two types of dispersion of components are distinguishable in such ternary systems: (1) the filler and the elastomer are separately dispersed in the matrix, and (2) the filler is encapsulated by the elastomer. In addition, many different morphologies with various extents of encapsulation are also possible. The effect of such differences of morphology on the mechanical properties also varies with the components used in the ternary composite systems. In some studies, it has been found that the encapsulated morphology produced a decrease in modulus but an increase in impact strength.[1–6] Such behavior was explained by the formation of soft and elastic layers around the rigid filler particles, which was beneficial for the improvement of the impact strength by suitable modification of the stress distribution around the filler particles.[7] However, the modulus and impact strength for such ternary systems, with separated dispersions of elastomer and rigid filler, increased.[8–12] In PP/elastomer/calcium carbonate ternary composites, the observed increase in the modulus was explained as a contribution of separately dispersed rigid filler, and the increase in impact strength was attributed to the combined effect of the rigid filler and the elastomer in the reduction of the matrix ligament thickness and, thereby, the initiation of shear deformation in the matrix.[12] When the particles were close together, the stress field around the particles interacted considerably, which resulted in enhanced shear yielding. Recently, Hong Yang et al.[13] reported a supertoughened PP/ethylene–propylene–diene monomer (EPDM)/nano-SiO_2 ternary composite with an impact strength 2–3 times higher than a PP/EPDM binary blend and 15–20 times higher than pure PP. They attributed the improvement in impact strength to the formation of a filler network structure around elastomer domains, which reduced the effective interparticle distance to cause the percolation of a stress field and, thus, enhanced matrix shear yielding.

Correspondence to: A. K. Gupta (akgncute@hotmail.com).

The phase dispersion of three-component composites is influenced by the interfacial tension between the components, the melt rheology, the processing technique, and the mixing sequence.[14,15] Thermodynamic considerations, such as interfacial tension, adhesive work, and wetting coefficient, are used to predict the phase morphology in ternary composites.[16] In this article, we present a study on a ternary system comprising PP as matrix, polydimethylsiloxane (PDMS) as an elastomer, and hydrophilic fumed nano-SiO_2 as the dispersed phase component. Unlike the similar ternary composite, PP/EPDM/nano-SiO_2, studied recently by Yang et al.,[13] this system, PP/PDMS/nano-SiO_2, had a greater affinity between the elastomer and the filler component because of the similarity of the chemical structures containing Si—O groups. Another reason for the selection of PDMS elastomer in this study was its suitability for high-temperature applications and its resistance to oxidation. Three different mixing sequences were used in this study during twin-screw compounding to produce the ternary composites, which were found to differ in dispersion morphology. The observed differences in dispersion morphology were correlated with the mechanical properties of the composites and the crystallization behavior of the PP matrix.

EXPERIMENTAL

Materials

The PP used in this study was a homopolymer, Repol H200MK, produced by Reliance Industries, Ltd. (Mumbai, India, melt flow index = 20 at 230°C/2.16 kg). The nano-SiO_2 used consisted of hydrophilic fumed silica nanoparticles supplied by Wacker Chemie AG (Munich, Germany) under the trade name Wacker HDK N 20. It had a surface area of 200 m^2/g. The particle sizes of the water suspension of nano-SiO_2 were determined with a Brookhaven 90 Plus particle size analyzer (Holtsville, NY) working on the principle of dynamic light scattering. The particle sizes were in the range 100 to 500 nm with mean and median diameters of 261 and 232 nm, respectively. The PDMS elastomer used was noncommercial grade (Silpren V-SS) with no filler or additive obtained from GE Bayer Silicones (Bangalore, India). The average molecular weight of PDMS, as determined by the viscosity method, was 250,000 on the basis of k and a values[17] calibrated with weight-average molecular weights.

Melt mixing and injection molding

The ternary composites were prepared in a twin-screw extruder made by Japan Steel Works, Ltd. (Tokyo, Japan) (JSW J75E IV-P) with a length/diameter ratio of 36 and a diameter of 30 mm. The materials were predried in a vacuum oven at 70°C for 3 h before blending. Extrusion was performed at a screw speed of 200 rpm, with the temperature profile 140–150–190–205–205–205–215–215–225–230°C from the feed zone to the die zone. The extruded strands were quenched in a water bath and granulated. The granules were then dried in a vacuum oven at 70°C for 2 h and injection-molded with a Demag L&T injection molding machine (model PFY 40), (L&T-Demag Plastics Machinary Pvt. Ltd., Chennai, India). The barrel temperature profile of the injection molding was 190–220–225–230°C, and the mold was at room temperature.

Three different mixing protocols were used to produce three different series of samples of the PP/PDMS/nano-SiO_2 ternary composites:

1. Two step mixing by the addition of nano-SiO_2 in the second step: these samples are designated with the prefix F followed by a number 2 to 8, which denotes the weight percentage of nano-SiO_2 filler in each 20-phr PP/PDMS blend.
2. One-step mixing: these samples are designated with the prefix W followed by a number 2 to 8, which denotes the weight percentage of the nano-SiO_2 filler.
3. Two-step mixing by the addition of PDMS in the second step: these samples are designated with the prefix P followed by a number 2 to 8, which denotes the weight percentage of nano-SiO_2 filler, with the PP/PDMS ratio identical with the F- and W-series samples (i.e., 20-phr PP/PDMS blend).

The sample nomenclature and composition are summarized in Table I. PP/nano-SiO_2 binary systems with 2–8 wt % filler were also made and tested under similar conditions to serve as references.

Morphology

The dispersion morphology of cryogenically fractured surfaces was investigated with scanning electron microscopy (SEM; EVO 50, Ziess, Oberkochen, Germany) and transmission electron microscopy (TEM; CM 12, Philips, Eindhoven, The Netherlands; 120 kV) techniques. Samples for SEM were etched in toluene for 2 days to dissolve PDMS, and then, the dried fracture surfaces were sputter-coated with silver before scanning. Thin sections around 200 nm thick prepared by a cryogenic ultramicrotome technique were used for TEM observation.

Differential scanning calorimetry (DSC)

The nonisothermal crystallization thermograms were recorded on a PerkinElmer Pyris-7 differential scanning calorimeter (PerkinElmer, Waltham, MA) with the temperature calibrated with indium. Sample pieces of 5–6 mg cut from the injection-molded

TABLE I
Compositions of the PP/PDMS/Nano-SiO_2 Samples Prepared by the Three Mixing Protocols

Sample name	PP (wt %)	PDMS (wt %)	Nano-SiO_2 (wt %)
PP	100	0	0
PP/E20	83.3	16.7	0
F2	81.7	16.3	2
F4	80.0	16.0	4
F6	78.3	15.7	6
F8	76.7	15.3	8
W2	81.7	16.3	2
W4	80.0	16.0	4
W6	78.3	15.7	6
W8	76.7	15.3	8
P2	81.7	16.3	2
P4	80.0	16.0	4
P6	78.3	15.7	6
P8	76.7	15.3	8

specimens were used for DSC measurements. The samples were heated from room temperature to 200°C and held there for 2 min to eliminate the residual crystals and memory effects of the thermal and shear histories, and subsequently, the melt was cooled at cooling rate of 10°C/min to room temperature under a nitrogen atmosphere to record the crystallization exotherm.

Mechanical properties

The tensile properties were measured on a Zwick universal tester (model 2010) (Zwick USA LP, Kennesaw, GA) at a crosshead separation of 6 cm and a crosshead speed of 50 mm/min, according to the ASTM D 638 type 1 test procedure.

Flexural properties were measured on the Zwick universal tester with a three-point bending system with center loading on a simply supported beam, in accordance with the ASTM D 790 test procedure.

The Izod impact strength of the notched specimens was determined on a falling hammer type Ceast impact meter (CEAST USA Inc., Charlottec, NC) according to the ASTM D 256 test method. The impact energy value obtained was divided by the thickness of the specimen (4 mm) and expressed in Joules/meter.

RESULTS AND DISCUSSION

Dispersion morphology

SEM micrographs of the binary system PP/PDMS (sample PP/E20), shown in Figure 1, indicated a sufficiently homogeneous dispersion of PDMS domains in the PP matrix.

The SEM micrographs of the F-series ternary composites, presented in Figure 2, showed an encapsulation of the nano-SiO_2 particles within PDMS domains. The encapsulated nano-SiO_2 particle are in agglomerated form. This encapsulation was observed in all samples with 2–8 wt % nano-SiO_2 content, with increasing encapsulation with increasing nano-SiO_2 content. The elastomer domains became enlarged and were distorted by the encapsulation.

The SEM micrographs of the W-series ternary composites, presented in Figure 3, showed a separated dispersion of the PDMS and nano-SiO_2 phases in the PP matrix. The fineness of the dispersion of PDMS varied, depending on the nano-SiO_2 content of the composite. The dispersion of nano-SiO_2 was not very uniform. The presence of nano-SiO_2 particles surrounding the PDMS domains and the occurrence of some agglomerates of nano-SiO_2 were seen in these ternary composites prepared by one-step mixing. A magnified view of the nano-SiO_2 particles surrounding a PDMS domain is shown in Figure 4(a), and in a further magnified view of the small region indicated by the rectangular area in Figure 4(a), shown in Figure 4(b), individual fine particles of nano-SiO_2 were seen. The formation of a fine band of nano-SiO_2 particles around the PDMS domains could have been due to the affinity of PDMS and nano-SiO_2 because of their similarity in chemical structure and the possibility of hydrogen bonding between the oxygen atom in the PDMS molecular chain and the surface hydroxyl groups of nano-SiO_2. Because of this affinity, some filler particles could even diffuse into the elastomer domains. However, evidence of an encapsulated morphology was negligible; the TEM micrographs of these composites, shown in Figure 5, revealed the presence of some nano-SiO_2 particles inside the elastomer domains. Thus, we can state that the one-step mixing of all three components, PP, PDMS, and the filler, used for the W series of samples, showed separate dispersion with a small degree of encapsulation and the surrounding of PDMS by nano-SiO_2 particles.

The dispersion morphology of the P-series ternary composites, prepared by the addition of PDMS to the already prepared PP/nano-SiO_2 composite, is

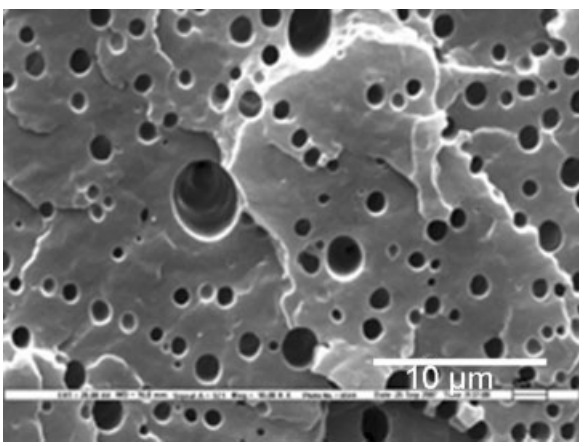

Figure 1 SEM micrograph of PP/PDMS blend sample PP/E20.

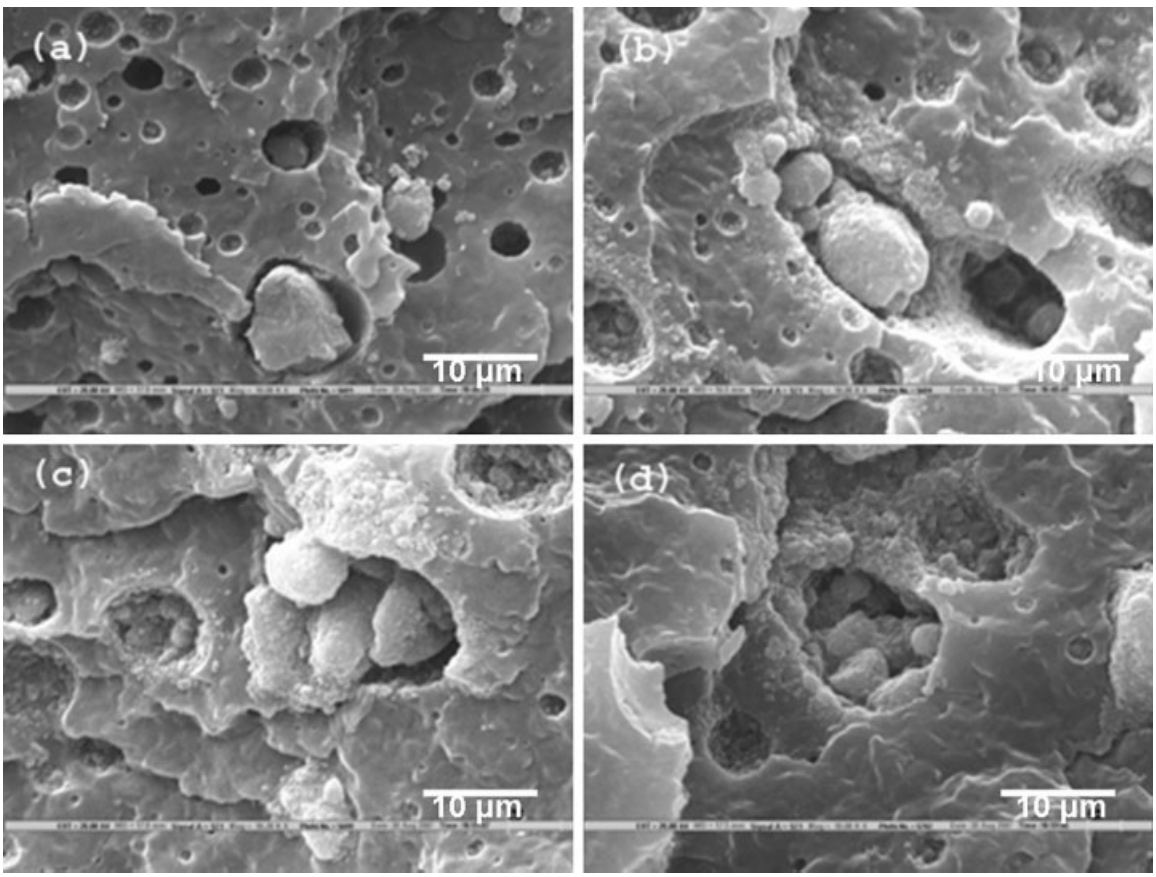

Figure 2 SEM micrographs of PP/PDMS/nano-SiO_2 ternary composite (F-series) samples: (a) F2, (b) F4, (c) F6, and (d) F8.

shown in Figure 6. An independent dispersion of the PDMS and nano-SiO_2 phases was present without, or with very little, encapsulation. The PDMS domains were finer in the P-series samples than in both the F- and W-series samples of the ternary composite, which indicated some role of the PP/nano-SiO_2 binary system in the dispersion of the PDMS elastomer. Nano-SiO_2 particles surrounded the PDMS domains in the form of a loose network, which was more prominent at higher nano-SiO_2 contents. Such a tendency of nano-SiO_2 particles to surround the elastomer domains was also reported by Yang et al.[13] for a PP/EPDM/nano-SiO_2 ternary system prepared by two-step mixing. The difference in dispersion of PDMS in the PP/nano-SiO_2 binary system as compared to the dispersion of PDMS in PP alone, was apparent in the tendency of the nano-SiO_2 particles to assemble closer to the PDMS domain boundaries, whereas the domain sizes were unaffected.

Crystallization exotherms

The DSC crystallization exotherms of the ternary composites are presented in Figure 7(a–c). We accounted for the observed differences in the exotherms by the differences in the morphology of dispersion. The crystallization exotherms of the F-series composites [Fig. 7(a)] showed a decrease in the onset and peak temperatures with increasing nano-SiO_2 content. Because of the predominance of encapsulated morphologies in the F-series ternary composites, little variation in the exotherm or crystallization behavior of PP was observed. On the other hand, in the W- and P-series ternary composites, both the onset and peak temperatures of crystallization exotherm increased with increasing nano-SiO_2 content. This was due to the presence of independently dispersed nano-SiO_2 particles, which were free to come in contact with the PP matrix in both the P- and W-series ternary composites. The nano-SiO_2 acted as a nucleating agent, which thus caused the increases in the onset and peak temperatures of the crystallization exotherm. The effect of nano-SiO_2 on the crystallization of PP is presented through the exotherms for the PP/nano-SiO_2 binary systems containing 0, 2, 4, 6, and 8 wt % nano-SiO_2 in Figure 8. As shown in Figure 8, the presence of nano-SiO_2 enhanced the nucleation of PP. The absence of such a nucleating effect in the F-series samples of the ternary composite was clear evidence of the inhibition of this nucleating role of nano-SiO_2 because of the encapsulation of nano-SiO_2 by the elastomer phase.

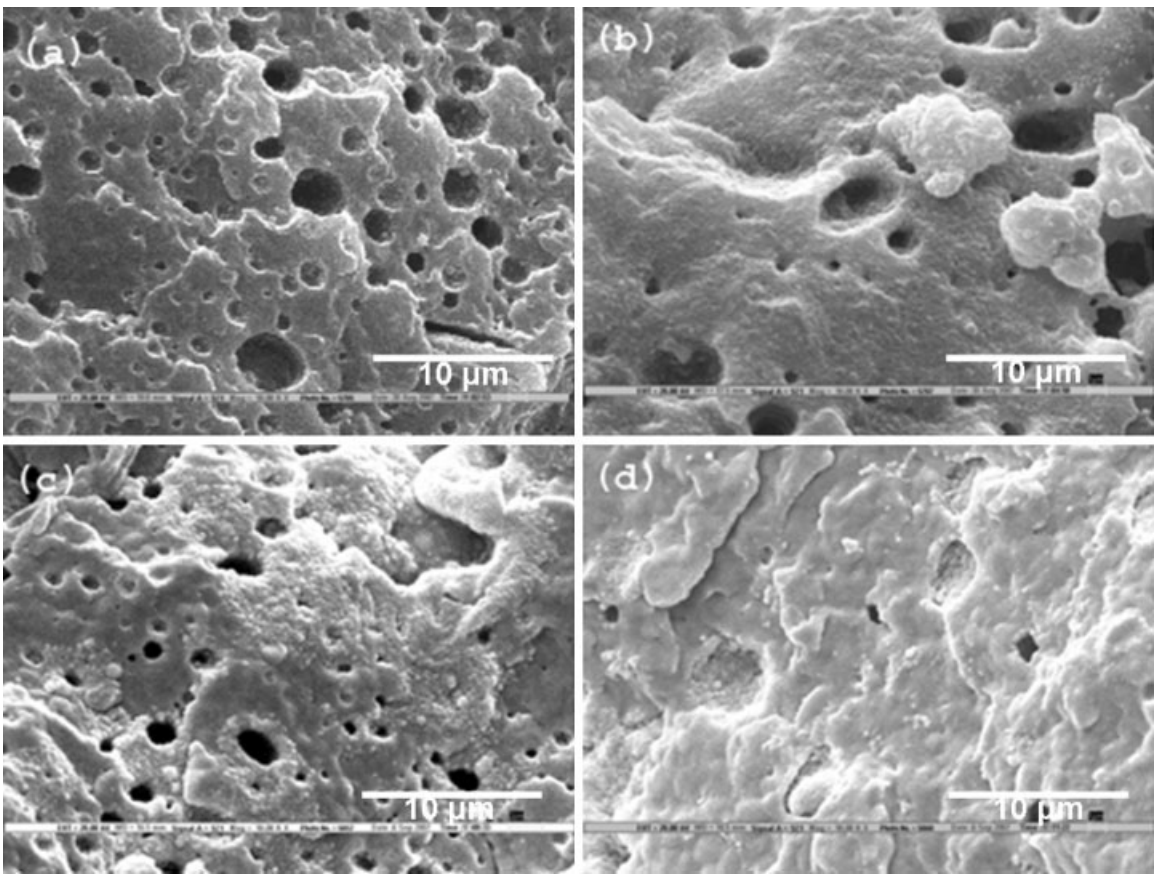

Figure 3 SEM micrographs of PP/PDMS/nano-SiO_2 ternary composite (W-series) samples: (a) W2, (b) W4, (c) W6, and (d) W8.

Mechanical properties

Stress–strain behavior

The stress–strain curves of these three sets of the ternary composites are presented in Figure 9(a–c). All of the samples showed yielding and a horizontal plateau region corresponding to the shear deformation of the PP matrix. In the binary system (sample PP/E20), shown by a solid line curve in Figure 9, the yield drop point was followed by a short horizontal plateau region. The reason for the short horizontal region was the high drawing and elongation occurring only at the small-necked region, rather than in the entire length of the specimen, which caused a long horizontal plateau

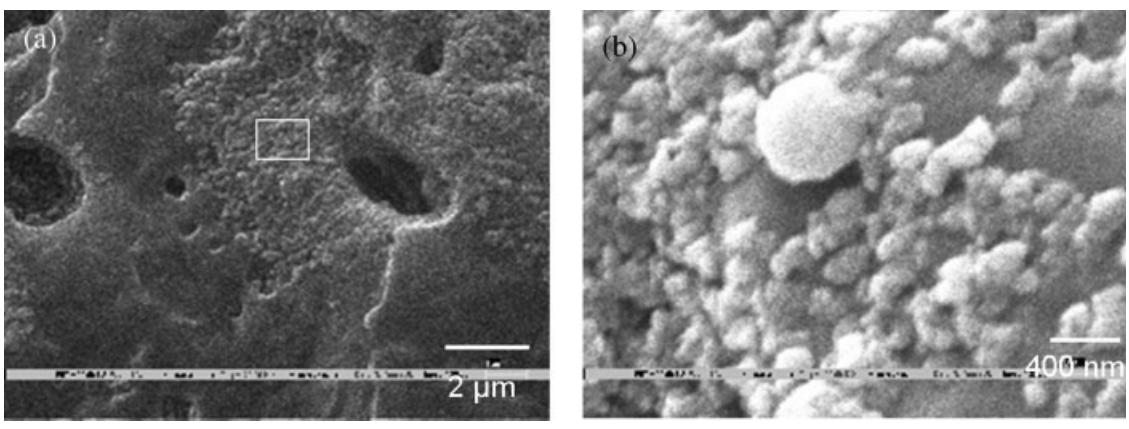

Figure 4 SEM micrographs of a PP/PDMS/nano-SiO_2 ternary composite (sample W4): (a) a finely dispersed band of nano-SiO_2 particles surrounding elastomer domains and (b) a magnified image of the small rectangular area in part a.

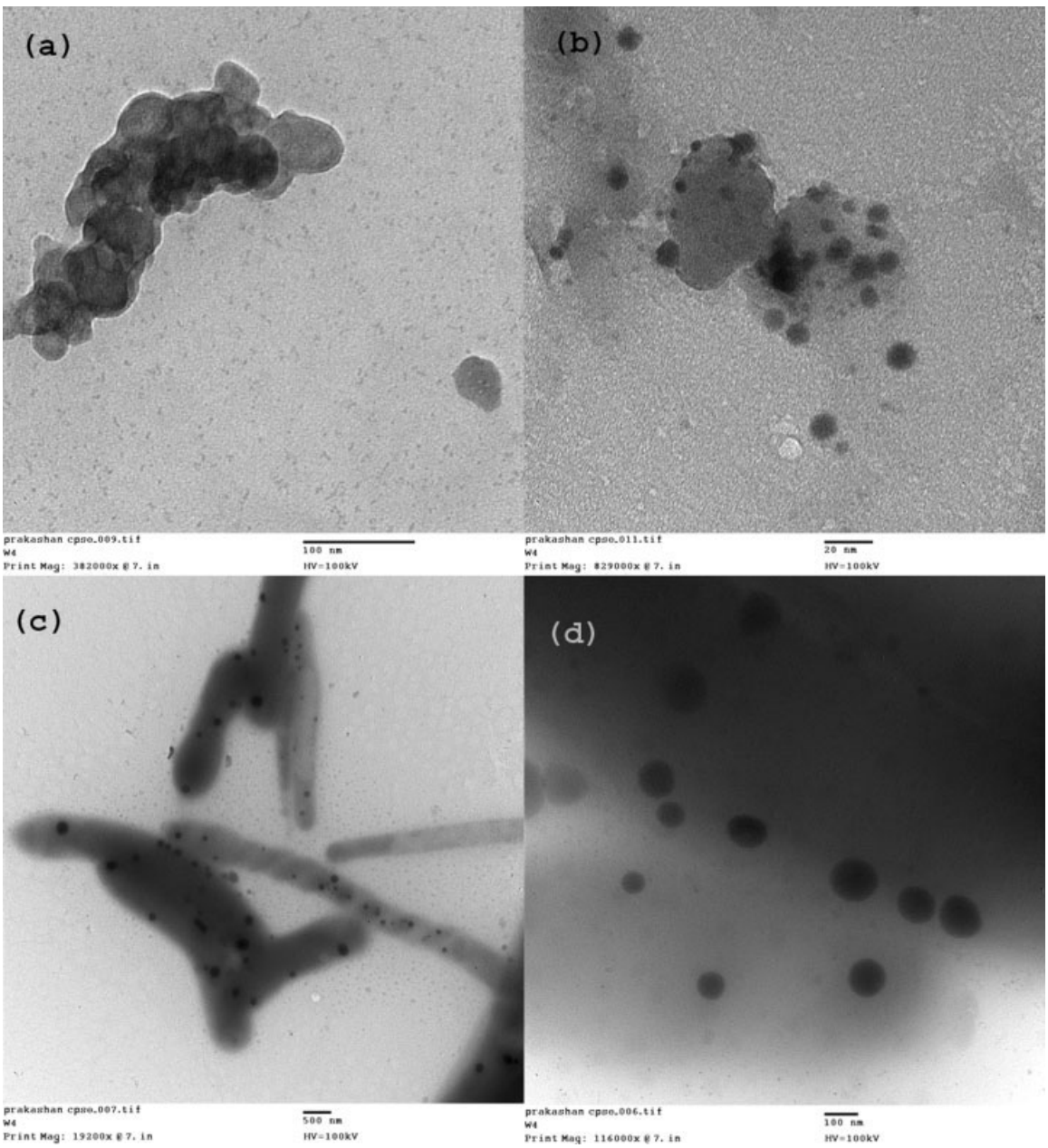

Figure 5 TEM micrographs of a PP/PDMS/nano-SiO_2 ternary composite (sample W4): (a) agglomerated nano-SiO_2 particles and (b–d) nano-SiO_2 particles inside elastomer domains.

region. After the short horizontal plateau, the stress decreased gradually with increasing strain, and after almost 60% elongation, the decrease in stress became very sharp, which finally led to breaking at about 100% elongation. This behavior was due to the fibrillation occurring in this binary system during tensile elongation. After the yield point, necking occurred, and the neck started elongating on further increase of strain. During this cold-drawing process, molecules oriented along the draw direction. The lubricating effect produced by PDMS facilitated cold drawing and resulted in the formation of microfibrils. These microfibrils started breaking, and the cross section of the elongating portion gradually decreased with continuing elongation of the specimen; finally, at a small cross section of the specimen, breaking occurred at a very low value of stress. This fibrillation behavior of the PP/PDMS blend was illustrated in our earlier article,[18] which showed the complete absence of such fibrillation in the PP/PDMS/nano-SiO_2 ternary composite.

In the F-series ternary composites, prepared by the addition of the nano-SiO_2 as a second step of compounding, the horizontal plateau region of the stress–strain curve was larger than that of the unfilled PP/E20 blend. The horizontal plateau decreased in length with increasing nano-SiO_2

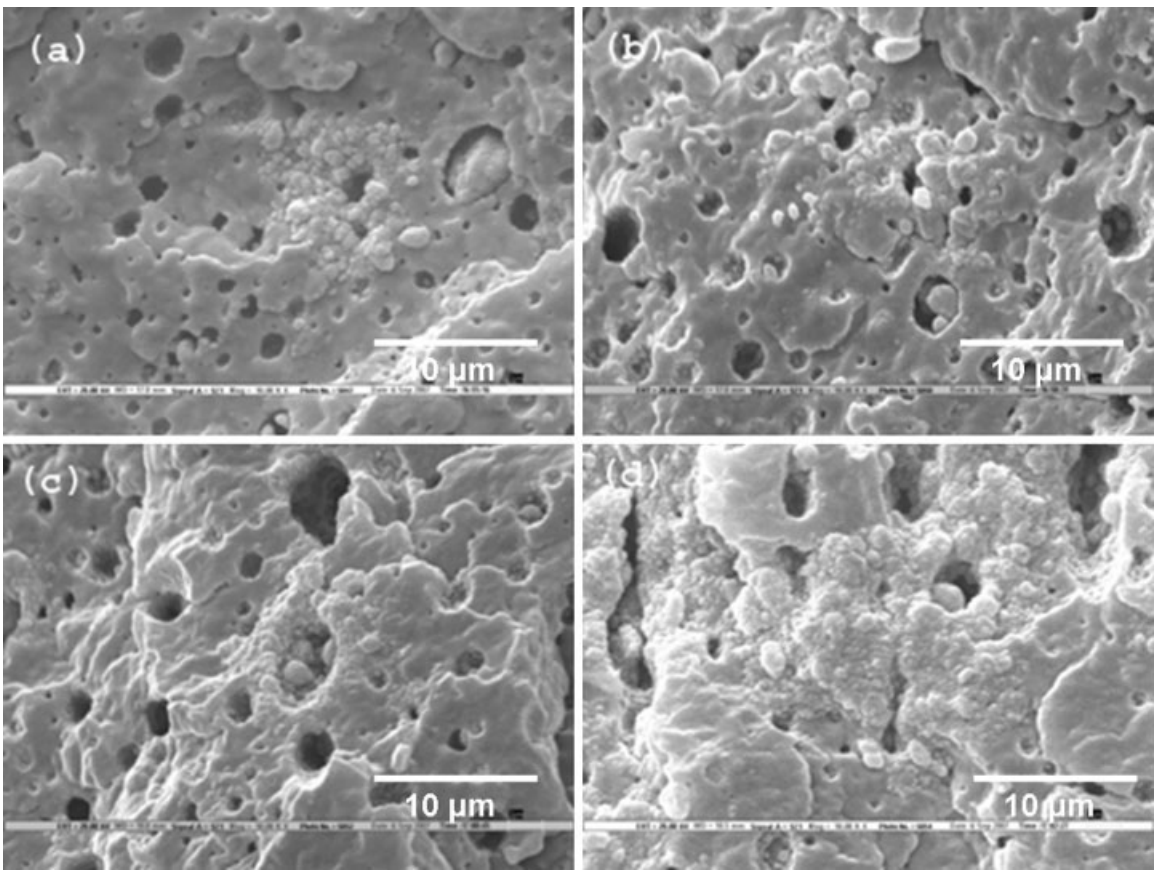

Figure 6 SEM micrographs of PP/PDMS/nano-SiO_2 ternary composite (P-series) samples: (a) P2, (b) P4, (c) P6, and (d) P8.

content in the F-series samples. This may have been due to fact that the dispersion morphology comprised encapsulated nano-SiO_2 particles, which may have restricted the deformations of the elastomer domains and, thus, prevented very high drawing of the small localized region and, thereby, produced small amounts of drawing in the entire length of the specimen. As the filler content increased, the encapsulation also increased, and this further restricted the deformation of PDMS domains, which caused a decrease in the overall elongation of the specimen at higher filler loadings.

In the W-series ternary composites, prepared by the one-step mixing of all three components, the horizontal plateau region was very short at the lowest and highest filler loading specimens (i.e., W2 and W8), whereas at 4 and 6 wt % filler loadings, this plateau was quite long. The dispersion morphology in the W-series ternary composite showed the presence of nano-SiO_2 particles on the periphery of elastomer domains along with some independently dispersed large agglomerates of nano-SiO_2. The presence of the nano-SiO_2 dispersion on the interface could have restricted the deformation of elastomer domains during the elongation of the specimen. In a previous study,[18] we illustrated the role of voiding (or debonding) at the elastomer matrix interface as the precursor for the activation of shear yielding in a PP/PDMS binary blend. Such restriction on the deformation of elastomer domains may prevent high elongation at localized points and, thus, cause small shear deformations to occur throughout the specimen, which may have added up to account for the increase in strain as seen by the plateau in the stress–strain curve of this set of ternary composites. At a very high filler loading (sample W8, which incidentally overlapped with the curve of sample W2), the extremely low breaking strain may have been due to the presence of a high proportion of independently dispersed large agglomerates of nano-SiO_2, which may have acted as stress concentrators to cause early breakage of the specimen.

In the P-series ternary composites, prepared by a two-step mixing sequence involving elastomer addition as second step, the horizontal plateau region was quite short at the lowest nano-SiO_2 filler content (2 wt %), and it increased with increasing filler content, and the maximum elongation, about 180%, was observed at the highest filler content (i.e., 8 wt %, sample P8). This behavior was explainable on the basis of dispersion morphology in this series of the ternary composite. A separate dispersion of PDMS

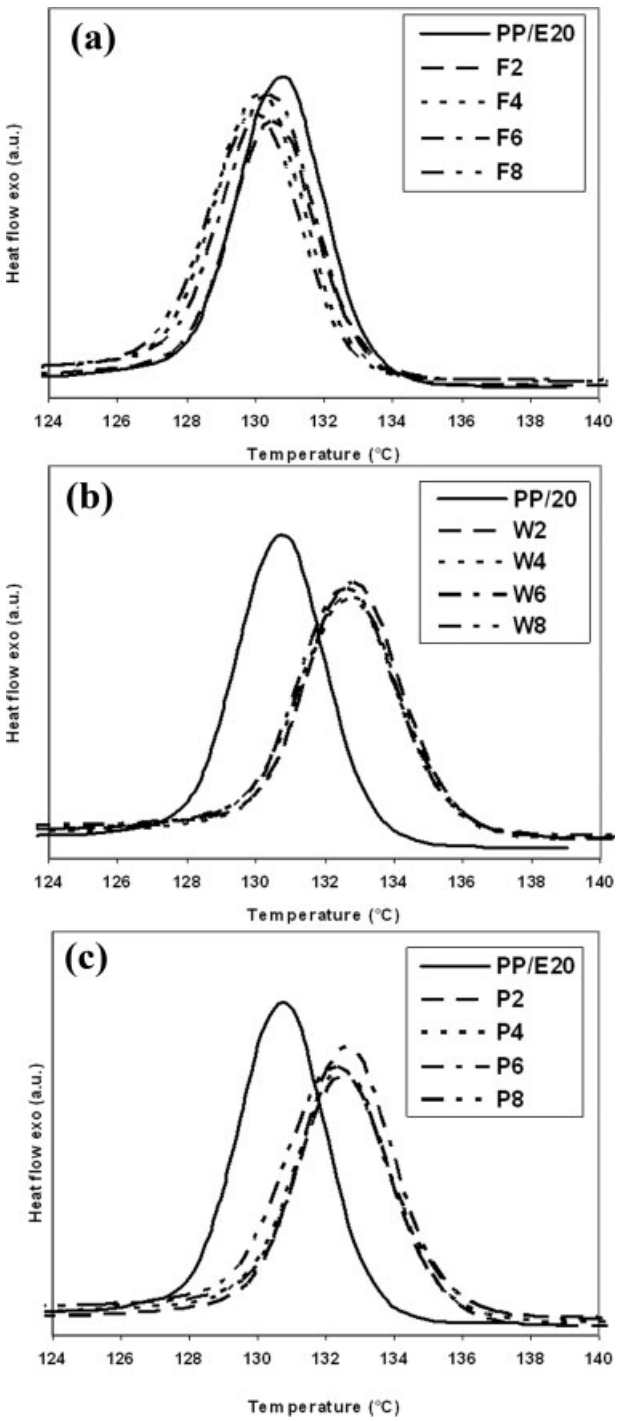

Figure 7 DSC crystallization exotherms of PP/PDMS/nano-SiO_2 ternary composites prepared with different mixing sequences: (a) F series, (b) W series, and (c) P series.

and nano-SiO_2 were present with a very fine dispersion of PDMS, compared to those of the F and W series. At low nano-SiO_2 content, the filler particles loosely surrounded some of the PDMS domains. Such a loosely bound dispersion may have had little influence on the deformation of the PDMS domains. After the yield point, high drawing and elongation occurred at the small area of cross section in the neck region, and the samples fractured around 50% strain, without fibrillation. However, as the nano-SiO_2 content increased, close packing of the nano-SiO_2 and PDMS domains occurred throughout the specimens. Such a close packing of elastomer and rigid particulate filler may have helped in the percolation of the stress field, which in turn, caused an ease in the deformation in the entire gauge length of the specimen.

Tensile and flexural properties

The variation of tensile strength with nano-SiO_2 content for the ternary composite is shown in Figure 10, along with the data for the corresponding PP/nano-SiO_2 binary system as a reference. The tensile strength decreased with increasing filler content for the PP/nano-SiO_2 binary system. In the W- and P-series ternary composites, the tensile strength increased at the initial 2 wt % nano-SiO_2 content from its value for the unfilled binary system. At higher filler contents, the tensile strength decreased with increasing filler content. This behavior was attributed to the dispersion morphology, which showed largely separated dispersions of nano-SiO_2 and PDMS in the PP matrix for the W and P series. In the F-series ternary composites, the decrease in tensile strength with increasing nano-SiO_2 content was more rapid than in the W- and P-series samples. Furthermore, the value of tensile strength at any fixed value of the filler content was lower for the F-series samples than for the W- or P-series samples. The lower value of tensile strength of the F-series samples seemed to be a result of the encapsulated morphology present in the F-series ternary composite. The domain sizes of the encapsulated domains in the F-series samples was larger than the PDMS

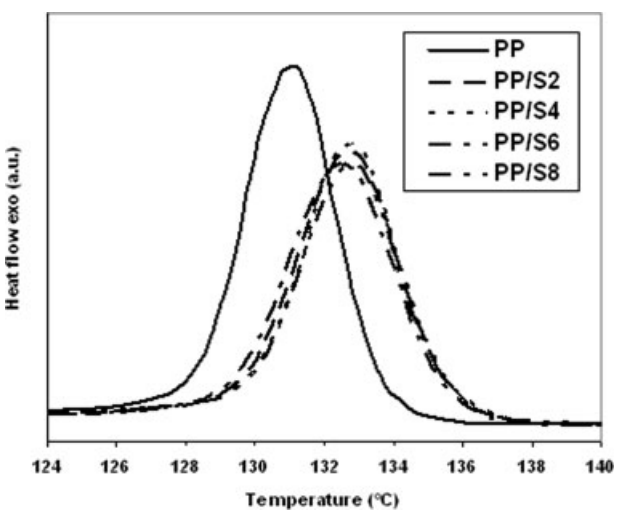

Figure 8 DSC crystallization exotherms of PP/nano-SiO_2 binary composites containing 2, 4, 6, and 8 wt % nano-SiO_2 (PP/S2, PP/S4, PP/S6, and PP/S8, respectively).

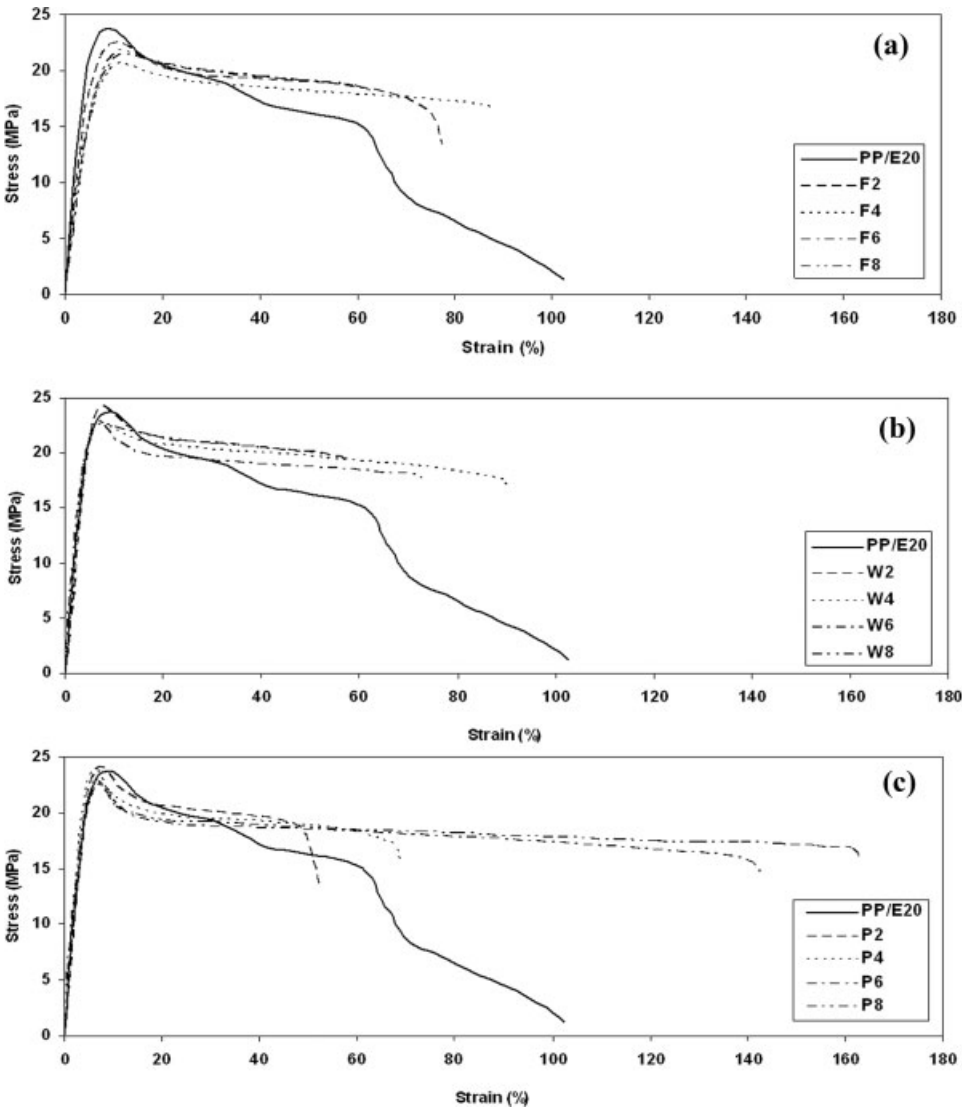

Figure 9 Stress–strain curves of PP/PDMS/nano-SiO$_2$ ternary composites: (a) F series, (b) W series, and (c) P series.

domains in the W and P series (Fig. 2), which may have accounted for large discontinuities in the stress transfer in the F-series samples, which hence, accounted for their poor tensile strength.

The variation in tensile modulus with nano-SiO$_2$ content for the ternary composites is shown in Figure 11, along with the data for the corresponding PP/nano-SiO$_2$ binary system, as a reference. The tensile modulus increased with increasing filler content for the PP/nano-SiO$_2$ binary system. In the ternary composites, the trend of variation of tensile modulus with filler content was quite different from that of the reference PP/nano-SiO$_2$ binary system. In the W- and P-series ternary composites, the tensile modulus increased with the initial 2 wt % addition of nano-SiO$_2$ from its value of 0% filler, and thereafter, at higher filler contents, it decreased with increasing filler content and retained a higher value than at 0% filler content. On the other hand, in the F-series ternary composites, the tensile modulus decreased sharply with the addition of nano-SiO$_2$ filler, and the F-series samples showed significantly lower values than the W- and P-series samples at each identical filler content. This reduced tensile modulus for the F-series ternary system was also attributable to the encapsulated dispersion morphology comprising the nano-SiO$_2$ filler.

The variation of flexural strength with nano-SiO$_2$ content for the ternary composite is shown in Figure 12, along with the data for the corresponding PP/nano-SiO$_2$ binary system, as a reference. The flexural strength of the PP/nano-SiO$_2$ binary system increased with the initial 2 wt % addition of nano-SiO$_2$ from its value at 0% filler, which was followed by a decrease at higher nano-SiO$_2$ contents, with a higher value retained than that at 0% filler content. In the W and P series, the flexural strength increased with the initial 2 wt % addition of nano-SiO$_2$ from its value at 0% filler, which was followed by a decrease at higher filler

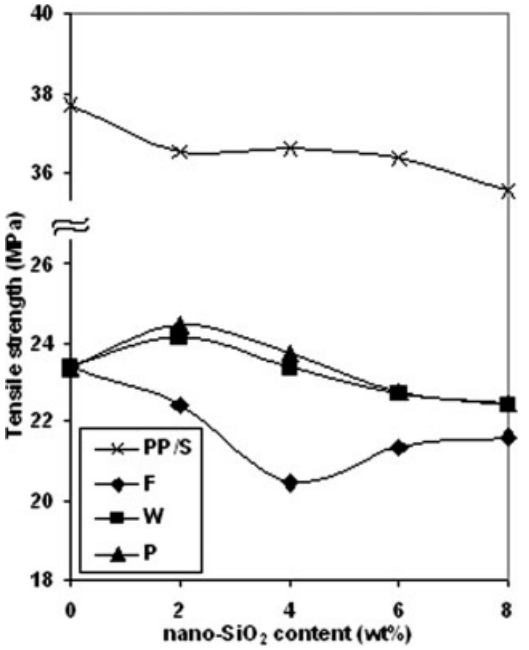

Figure 10 Variation of the tensile strength with the nano-SiO_2 content for the three series of ternary composites (F, W, and P) and the PP/nano-SiO_2 binary system (PP/S).

contents, with a higher value retained than that at 0% filler content. In the F-series ternary composite, the flexural strength decreased continuously with filler content, with values for the F series being much lower than the values for the W or P series at each identical nano-SiO_2 content. This was attributable to the encapsulated morphology of the nano-SiO_2 particles in the F-series ternary composites.

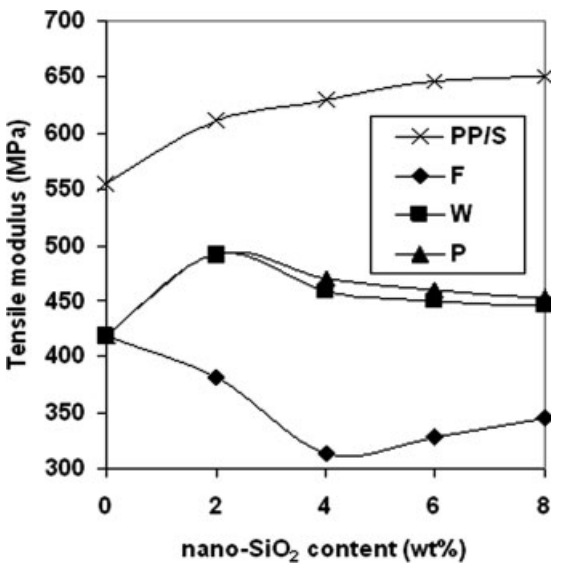

Figure 11 Variation of the tensile modulus with the nano-SiO_2 content for the three series of ternary composites (F, W, and P) and the PP/nano-SiO_2 binary system (PP/S).

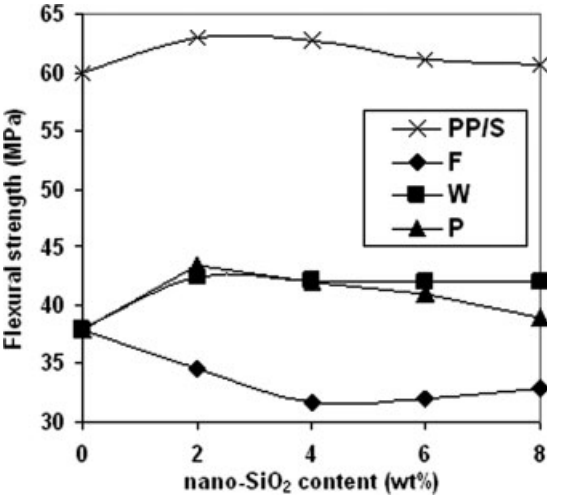

Figure 12 Variation of the flexural strength with the nano-SiO_2 content for the three series of ternary composites (F, W, and P) and the PP/nano-SiO_2 binary system (PP/S).

The variation of flexural modulus with nano-SiO_2 content for the ternary composite is shown in Figure 13, along with the data for the corresponding PP/nano-SiO_2 binary system, as a reference. The flexural modulus of the PP/nano-SiO_2 binary system increased continuously with filler content, whereas for the W- and P-series ternary composites, which had separated dispersions of nano-SiO_2, the flexural strength increased with the initial 2 wt % addition of nano-SiO_2 from its value at 0% filler, which was followed by a decrease at higher filler contents. However, in the F-series ternary composite, which had an encapsulated morphology, a larger decrease in the flexural modulus was observed. This indicated that

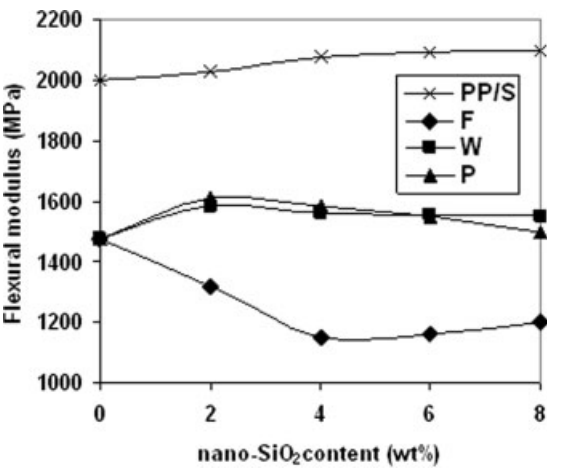

Figure 13 Variation of the flexural modulus with the nano-SiO_2 content for the three series of ternary composites (F, W, and P) and the PP/nano-SiO_2 binary system (PP/S).

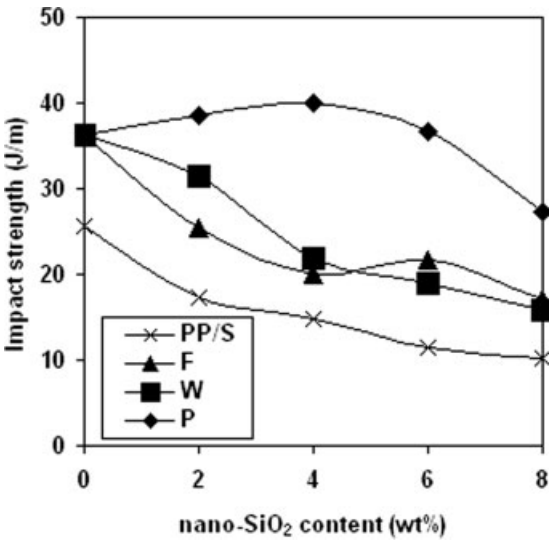

Figure 14 Variation of the impact strength with the nano-SiO_2 content for the three series of ternary composites (F, W, and P) and the PP/nano-SiO_2 binary system (PP/S).

the flexural modulus of the ternary system with an encapsulated morphology (F series) was much lower than that of systems with separated dispersions of nano-SiO_2 in the matrix (W and P series).

Impact strength

The variation of impact strength with nano-SiO_2 content for the ternary composite is shown in Figure 14, along with the data for the corresponding PP/nano-SiO_2 binary system, as a reference. The impact strength of PP decreased with increasing nano-SiO_2 content.

With the addition of 20-phr PDMS (i.e., sample PP/E20) the impact strength of PP increased from 26.6 to 36.2 J/m. This increase was somewhat lower than the increases in various rubber-toughened PP systems.[19,20] In a previous study[18] on a PP/PDMS system, we attributed this low improvement of impact strength to debonding at the elastomer–matrix interface, which could have facilitated crack propagation through the boundary of the elastomer domains.

In both the F and W series, the impact strength decreased with increasing nano-SiO_2 content. The values of impact strength were lower for F-series samples than for the W-series samples at 2–4 wt % filler content. In the F-series ternary composite, a large amount of nano-SiO_2 filler particles were encapsulated inside the elastomer domains, and this restricted the deformability of the domains, which is necessary for rubber-toughening mechanisms. However, in the W series, the encapsulation is lower, and

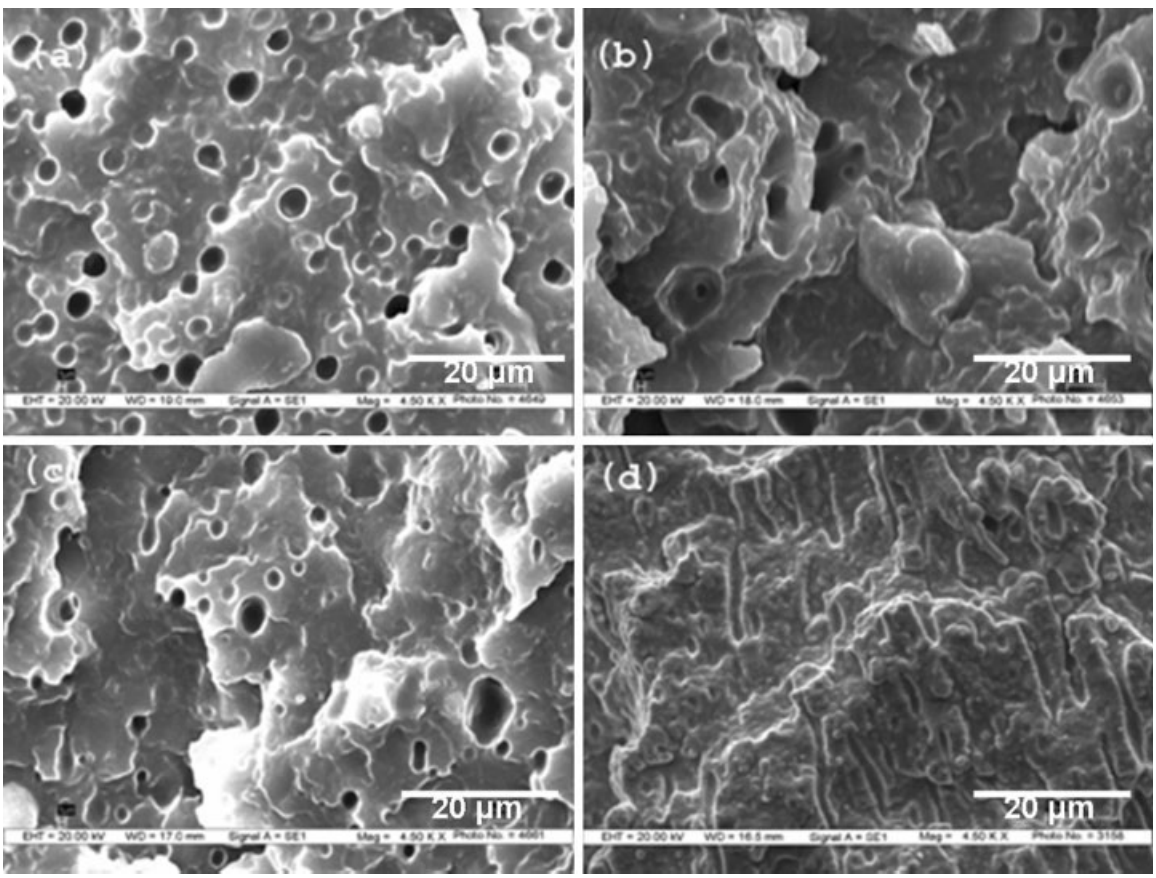

Figure 15 SEM micrographs of impact-fractured surfaces of various samples: (a) the PP/E20 blend, (b) F4, (c) W4, and (d) P4.

therefore, the elastomer domains may have acted differently from those containing nano-SiO_2 within them. Hence, the values of impact strength for the W series were higher than those for the F series. However, at higher nano-SiO_2 contents (i.e., at 6 and 8 wt %), the effects of the filler dominated, and thus, the impact strength of the W series was lower than that of the F series. The impact strength of the P-series samples was much higher than that of the F- and W-series samples at each identical nano-SiO_2 content. The expected role of nano-SiO_2 in the production of a decrease in the impact strength with increasing filler content seemed to reverse at low filler contents (2–4 wt %) in the P-series samples, whereas at higher filler contents (i.e., >6 wt %), the impact strength decreased with increasing filler content. The increase in impact strength with increasing nano-SiO_2 content (at 2–4 wt %) for the P-series samples seemed to be the effect of a smaller size of elastomer domain in the P series at 2 and 4 wt % filler contents than in the F and W series (see Figs. 2, 3, and 6 for comparisons). It is likely that the mean sizes of the elastomer domains at 2 and 4 wt % filler contents were within the range of critical elastomer particle size required for the impact toughening of PP/PDMS. The improvement in impact strength was not much, which indicated that the role of nano-SiO_2 in decreasing the impact strength was simultaneously operative.

The SEM micrographs of the impact-fractured surfaces of the samples of the ternary composites and PP/E20 binary blend are shown in Figure 15. For the PP/E20 blend sample [Fig. 15(a)], the micrograph showed fracture through elastomer boundaries. This indicates that debonding at the elastomer matrix interface might have facilitated crack propagation through elastomer boundaries, and this accounted for the low value of impact strength for the PP/E20 binary blend. The fracture surface of the F-series sample (F4) [Fig. 15(b)] showed the presence of large voids, which may have been due to the pullout of large encapsulated elastomer domains during fracture. The fractured surface of the W-series sample (W4), shown in Figure 15(c), indicated a brittle facture with fracture through elastomer domains. In the P-series sample P4 [Fig. 15(d)], shear deformation leading to the elongation of the elastomer domains was seen. As already explained, this shear yielding, which accounted for the additional mechanism of energy dissipation, may have been the reason for the observed higher impact strength of the P-series composites.

CONCLUSIONS

The mixing protocol influenced the dispersion morphology of PP/PDMS/nano-SiO_2 ternary composites and, thereby, produced changes in the mechanical properties and crystallization behaviors. A one-step mixing sequence in all of these components (W series) resulted in a predominantly separated dispersion of the PDMS and nano-SiO_2 phases in the PP matrix, with some nano-SiO_2 particles forming a fine band surrounding the elastomer domains, whereas a few of them got encapsulated inside the PDMS domains. A two-step mixing sequence, where the nano-SiO_2 was added in the second step (F series), resulted in the predominant encapsulation of nano-SiO_2 by PDMS. The third protocol of mixing, which involved two-step mixing by the addition of PDMS in the second step (P series), resulted in a predominantly separated dispersion of nano-SiO_2 and PDMS in the PP matrix.

The separated dispersion morphologies showed higher values of tensile and flexural properties than that of the ternary composites with an encapsulated dispersion morphology. The impact strength of the ternary systems decreased with increasing nano-SiO_2 content regardless of the dispersion morphology, except at low nano-SiO_2 contents ($\leq$4 wt %) for the P-series ternary system. The impact strength of the P-series ternary system (where the elastomer was added in the second step of mixing) showed distinctly superior impact strength to the other two series (W and F) of samples. The fracture surface morphology showed evidence of shear yielding. The crystallization behavior of the PP matrix was affected more significantly in the morphology where nano-SiO_2 particles were dispersed in the matrix than in the encapsulated morphology.

References

1. Hornsby, P. R.; Premphet, K. J Appl Polym Sci 1998, 70, 587.
2. Kolarik, J.; Lednicky, F.; Jancar, J.; Pukanszky, B. Polym Commun 1990, 31, 201.
3. Long, Y.; Shanks, R. A. J Appl Polym Sci 1996, 61, 1877.
4. Stricker, F.; Mulhaupt, R. J Appl Polym Sci 1996, 62, 1799.
5. Dubnikova, I. L.; Berezina, S. M.; Antonov, A. V. J Appl Polym Sci 2002, 85, 1911.
6. Li, Z.; Guo, S.; Song, W.; Hou, B. J Mater Sci 2003, 38, 1793.
7. Lu, S.; Yan, L.; Zhu, X.; Qi, Z. J Mater Sci 1992, 17, 4633.
8. Premphet, K.; Horanont, P. J Appl Polym Sci 2000, 76, 1929.
9. Wang, J.; Tung, J. F.; Ahmad Fuad, M. Y.; Hornsby, P. R. J Appl Polym Sci 1996, 60, 1425.
10. Kolarik, J.; Jancar, J. Polymer 1992, 33, 4961.
11. Dekkers, M. E. J.; Dortmans, J. P. M.; Heikens, D. Polym Commun 1985, 26, 145.
12. Ling, Z.; Zhenghua, W.; Rui, H.; Liangbin, L.; Xinyuan, Z. J Mater Sci 2002, 37, 2615.
13. Yang, H.; Zhang, X.; Qu, C.; Li, B.; Zhang, L.; Zhang, Q.; Fu, Q. Polymer 2007, 48, 860.
14. Fisher, I.; Siegmann, A.; Narkis, M. Polym Compos 2002, 23, 34.
15. Dasari, A.; Yu, Z. Z.; Mai, Y. W. Polymer 2005, 46, 5986.
16. Ma, C. G.; Zhang, M. Q.; Rong, M. Z. J Appl Polym Sci 2007, 103, 1578.
17. Bandrup, J.; Immergut, E. H. Polymer Handbook, 2nd ed.; Wiley: New York, 1975; p IV–29.
18. Prakashan, K.; Gupta, A. K.; Maiti, S. N. J Appl Polym Sci 2007, 105, 2858.
19. Mehrabzadeh, M.; Hossein Nia, K. J Appl Polym Sci 1999, 72, 1257.
20. Zhao, R.; Dai, G. J Appl Polym Sci 2002, 86, 2486.